0425

RESPONSE BEHAVIOR OF PIPELINE SYSTEM SUBJECTED TO SUBSIDENCE OF GROUND LIQUEFACTION

Kunihiko FUCHIDA[1], Shozo SHIRINASHIHAMA[2] And Takashi AKIYOSHI[3]

SUMMARY

The purpose of this study is to investigate the effect of the compacting improvement method on the ground displacement of liquefied surface layers and the response behavior of buried pipeline subjected to such displacement. The authors develop the 2D FE analysis program for evaluating the ground subsidence during liquefaction including the compacting improvement case. Combining the programs for the simulation of the compacting method, the liquefaction analysis and the analysis of the ground subsidence, the responses of the pipeline subjected to the ground subsidence are analyzed. The numerical computational results of the liquefied ground and the pipeline show that the compacting improvement method is effective to reduce the responses of the surface ground and the pipeline.

INTRODUCTION

The responses of structures constructed at reclaimed lands or near shoreline in urban area are much affected by liquefaction of the surface ground layers during earthquakes. Permanent ground displacement or subsidence displacement induced by soil liquefaction is one of the most important problems for aseismic design of structures constructed in such ground layers possible to be liquefied [Hamada *et al.* 1986, 1995]. So far, there have been many examples of the sand compaction pile (SCP) construction as anti-liquefaction method in Japan, and the effects of SCP on soil liquefaction during past earthquakes have been verified in only several cases [JSCE, 1994, Yasuda *et al*. 1996].

We have proposed the analytical method for lateral flow displacement of liquefied ground, which is based on the effective stress analysis of the surface ground layers and the potential head method for inclined surface layers [Akiyoshi *et al*. 1998]. This method proved its efficiency by comparing with experimental results. In this paper we apply this analytical method to the analysis for the ground subsidence including the effect of the compacting ground improvement method against liquefaction. Finally the responses of the pipeline subjected to the subsidence of the surface ground are evaluated for the case of ground improvement.

ANALYTICAL METHODS

Liquefaction Analysis and Simulation of Ground Improvement

The authors have developed the evaluation system of anti-liquefaction improvement by SCP, which consists of the program [WAP3] (Wave Accumulation Process in 3-dimension) for simulation of SCP method [Akiyoshi *et al.* 1994] and 2D dynamic effective stress analysis program [NUW2] (Non-linear u-w analysis in 2-dimension) [Akiyoshi *et al.* 1993]. In WAP3, the decrement Δe_2 of the void ratio and the increment ΔG_2 of the stiffness of the sandy soils are assumed to be caused by the strain accumulation for the wave propagation due to the vibration in the compaction.

$$e = e_1 - \Delta e_2 , \quad G = G_1 + \Delta G_2 \tag{1}$$

[1] *Dept of Civil & Architectural Eng, Yatsushiro College of Technology, Japan E-mai fuchida@as.yatsushiro-nct.ac.jp*
[2] *Research Institute of Engineering, Tekken Kensetsu Corporation, Narita, JapanEmail: shozo-shirinashihama@tekken.co.jp*
[3] *Dep of Civil & Environmental Engineering, Kumamoto University, Kumamoto, JapanE-mail: akiyoshi@gpo.kumamoto-u.ac.jp*

where e, e_1 are the void ratios after and before improvement, respectively; G, G_1 are the shear moduli after and before improvement, respectively. In this process the following relations represented by the parameters as the fine content of sand, the vibrating forces, the spacing and the compacting time of SCPs are used;

$$e = (e_0 - e_{\min})e^{-Z} + e_{\min} \tag{2}$$

$$G = 900\frac{(2.17-e)^2}{1+e}(\sigma'_0)^{0.38} \tag{3}$$

where $Z=a\varepsilon^b N_n$; e_0, e_{min} are the initial and minimum void ratios, respectively; ε is the volumetric strain amplitude; N_n is the frequency of the dynamic compaction; a, b are the regression coefficients, b=0.75, and the coefficient a is expressed in terms of the fine content F_c(%) and the effective vertical pressure σ_v (kgf/cm^2);

$$a=10^{-1.126}(F_c/100/\sigma_v)^{-0.698} \tag{4}$$

The program NUW2 for the response analysis of the surface ground layer is based on the two-phase mixture theory of Biot [Zienkiewictz & Shiomi 1984] and the strain space multimechanism theory of soil as the constitutive equations [Iai *et al.* 1992]. A generalized Biot's governing equation and pore fluid equation are represented, respectively, as;

$$\mathbf{L}^T\sigma + \rho\mathbf{b} = \rho\ddot{\mathbf{u}} + \rho_f\ddot{\mathbf{w}} \tag{5}$$

$$-\nabla p + \rho_f\mathbf{b} = \rho_f\ddot{\mathbf{u}} + \frac{\rho_f}{n}\ddot{\mathbf{w}} + \frac{1}{k}\dot{\mathbf{w}} \tag{6}$$

where a superposed dot indicates a time derivative and a vector matrix notation is used to represent tensors; i.e.

$$\begin{aligned}
\boldsymbol{\sigma}^T &= (\boldsymbol{\sigma}_{xx}, \boldsymbol{\sigma}_{yy}, \boldsymbol{\sigma}_{zz}, \boldsymbol{\sigma}_{xy}, \boldsymbol{\sigma}_{yz}, \boldsymbol{\sigma}_{zx}) \\
\mathbf{u}^T &= (u_x, u_y, u_z), \quad \mathbf{w}^T = (w_x, w_y, w_z) \\
\mathbf{b}^T &= (b_x, b_y, b_z) \\
\boldsymbol{\varepsilon}^T &= (\partial/\partial x, \partial/\partial y, \partial/\partial z)
\end{aligned} \tag{7}$$

$$\mathbf{L}^T = \begin{bmatrix} \partial/\partial x & 0 & 0 & \partial/\partial y & 0 & \partial/\partial z \\ 0 & \partial/\partial y & 0 & \partial/\partial x & \partial/\partial z & 0 \\ 0 & 0 & \partial/\partial z & 0 & \partial/\partial y & \partial/\partial x \end{bmatrix} \tag{8}$$

where $\boldsymbol{u}$, $\boldsymbol{w}$ are the solid phase displacement and the relative pore fluid displacement, respectively; $\boldsymbol{\sigma}$ is the total stress; $\boldsymbol{b}$ is the body force; p is the pore fluid pressure; n is the porosity; ρ, ρ_f are the density of the bulk solid-fluid mixture and the density of the pore fluid, respectively, so that ρ = (1-n)ρ_s+$n\rho_f$, where ρ_s is the density of the solid grain; k is the isotropic permeability coefficient.

The stress-strain relationship of a linear, isotropic elastic material can be written as

$$\sigma = \mathbf{D}\varepsilon - \alpha\mathbf{m}p \tag{9}$$

$$p = -\alpha Q\mathbf{m}^T\varepsilon - Q\varsigma \tag{10}$$

where $\boldsymbol{\varepsilon}$=$\boldsymbol{Lu}$, $\boldsymbol{\zeta}$= $^T\boldsymbol{w}$ are the strain in the solid and the volumetric strain in the pore fluid, respectively; **D** is the drained material stiffness matrix; $\mathbf{m}^T$=(1,1,1,0,0,0) is equivalent to the Kronecker's delta; α, Q are related with materials through

$$\alpha = 1 - K_d/K_s, \quad 1/Q = n/K_f + (\alpha - n)/K_s \tag{11}$$

where K_s, K_f are the bulk moduli of the solid and pore fluid, respectively; K_d is the bulk modulus of the solid skeleton.

The program NUW2 evaluates the shear modulus and the excess pore water pressure ratio of the improved or un-improved ground. The details of the analytical procedure of [NUW2] and [WAP3] are shown in the papers [Akiyoshi *et al.* 1993 and 1994], and omitted here.

Analysis of Lateral Flow and Subsidence by Potential Head Method

We have proposed the analytical method for the lateral flow of liquefied ground, which is based on the static analysis for the shear deformation of 2D bi-linearly elastic ground model as shown in Figure 1 [Yasuda *et al.* 1992]. In this analysis the potential head of the inclined ground is added to the gravity force as the external one. It is also assumed that the shear modulus of the liquefied ground is reduced according to the reduction rate, which is related to the excess pore water pressure ratio as shown in Figure 2. This process has been developed to the 2D finite element static analysis program [FLOW] [Akiyoshi *et al.* 1998].

In this paper, we apply above analytical program to the analysis for the liquefied ground subsidence, because there are many pipeline damages caused by the subsidence as much as lateral flow displacement. Same relation between reduction rate and excess pore water pressure is also used in the analysis for the subsidence. Combining the program FLOW with WAP3 and NUW2, the coefficients of subgrade reaction and the subsidence of the SCP-improved or un-improved ground can be evaluated.

Analysis of Pipelines Buried in Liquefied Ground

The responses of pipelines subjected to the ground displacement induced by liquefaction are analyzed by the program [PIPE], which is based on the beam theory on an elastic foundation. Replacing the stiffness of liquefied ground around the pipeline with a coefficient of subgrade reaction, the pipeline is modeled as pipeline-soil spring system. The pipeline segments are connected by the axial and rotational joint springs k_t and k_r, respectively. The joint and soil springs are assumed to be bi-linearly elastic and the inertia and damping forces are neglected under the static load assumption. Based on these assumptions, the governing equilibrium equations

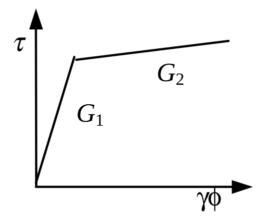

Figure 1: Relation Between Shear Stress And Shear Strain Of Liquefied Ground

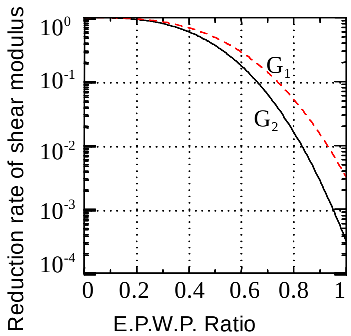

Figure 2: Reduction Rate Of Shear Modulus Of Liquefied Ground

of a small element are as follows;

$$-EA\frac{d^2u}{dx^2}+k_{sx}u=k_{sx}u_s \qquad \text{[Axial direction]} \qquad (12)$$

$$EI\frac{d^4v}{dx^4}+k_{sy}v=k_{sy}v_s \qquad \text{[Lateral direction]} \qquad (13)$$

where E, I, A are Young' modulus, moment of inertia and cross sectional area, respectively; k_{sx}, k_{sy} are soil spring per unit length for axial and lateral directions, respectively; u, v and u_s, v_s are axial, lateral displacements of pipe and ground, respectively. For solving the governing equilibrium equations in the axial and lateral directions and minimizing the accumulative errors in the numerical computations, the modified transfer matrix (MTM) method technique is adopted. For the details of the MTM method, readers are referred to the report [Fuchida *et al.* 1993].

RESULTS OF NUMERICAL COMPUTATIONS AND CONSIDERATIONS

Analytical results of subsidence of model ground

Figure 3 is the field scale ground model in which the ground improvement is performed by SCP. The ground model as shown in Figure 3 consists of the base layer (Thickness H_3), the saturated sandy layer (H_2) and the topsoil (H_1) with the initial N-value 7, and the thickness of each layers are assumed as shown in Table 1. As the relation between N-value and the shear modulus, the equation (14) is used [JRA, 1996].

$$V_s = 80N^{1/3} \tag{14}$$

where V_s is shear velocity of soil. The SCPs are constructed separating several blocks in which one block consists of triple lines of SCPs with the width 5m and the constructing condition is shown in Table 2. The liquefaction analysis is performed for the ground models subjected to El Centro Earthquake (1940) with the maximum acceleration 0.25G, then the ground subsidence is analyzed by the program FLOW.

Figure 4 shows the maximum subsidence of un-improved and SCP-improved cases of 5 ground models as shown in Table 1, in which black and white circle symbols show the subsidence of un-improved and SCP-improved cases, respectively. The subsidence displacement of un-improved case decreases, as the thickness of liquefied soil layer (H2 in Figure 3) becomes thin. If the thickness of the liquefied layer is about 10m, the subsidence response around 0.5m in Figure 4 is comparable with the average of the observed subsidence in Port Island during Hyougoken-Nanbu Earthquake [Yasuda *et al.* 1996]. After the ground improvement by the program WAP3 the initial N-value 7 of the ground increases to the N-value about 20. Thus the subsidence of the SCP-

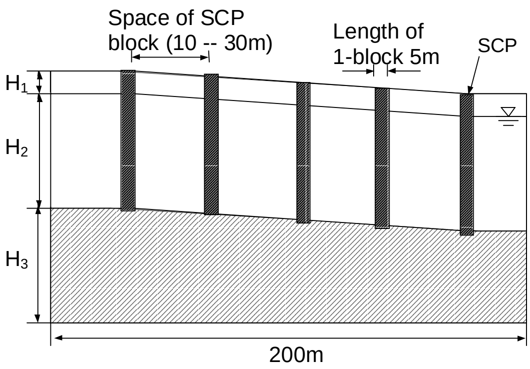

Figure 3: Ground Layers Model

Table 1: Thickness of layers

	Model 1	Model 2	Model 3	Model 4	Model 5
H1	3	3	3	3	3
H2	16m	14m	12m	10m	8m
H3	10m	10m	10m	10m	10m

Table2: Conditions of SCP method

Term	Conditions
Array	Rectangular
Space of piles (m)	2.0
Compacting force(kN)	591.9
Radius of sand pile (m)	0.4
Frequency (Hz)	9.3
Compacting time per 1 stage (sec	100

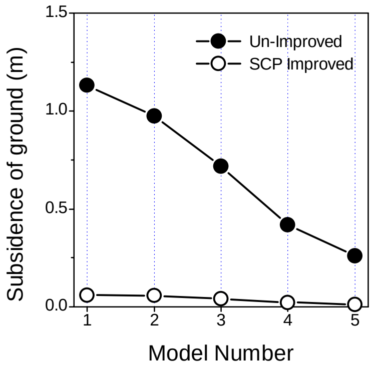

Figure 4: Maximum Ground Subsidence

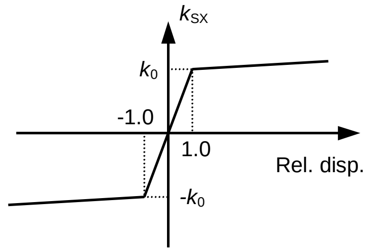

Figure 5: Characteristics Of Soil Spring

Table 3: Reference pipe parameters

Physical items	Values(unit)
Material of segment	Ductile cast iron
Nominal diameter	500 (mm)
Thickness	9.5 (mm)
Total length	100 (m)
Buried depth	2 (m)
Young modulus	$1.57\text{x}10^8$ (kN/m^2)
Specific gravity	7.15
Tensile strength	$3.92\text{x}10^5$ (kN/m^2)
Bending strength	$5.59\text{x}10^5$ (kN/m^2)
Allowable joint expansion	50 (mm)
Allowable joint rot. angle	5 (degree)

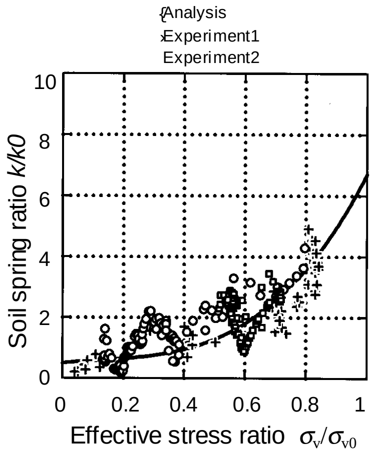

Figure 6: Relation Between Soil Spring Ratio

improved case is much smaller than that of un-improved case, which suggests that the SCP-improvement is effective on preventing liquefaction of the ground and reducing displacement of it during earthquake.

Numerical conditions for pipeline analysis

The pipeline parameters used in the numerical computations are shown in Table 3. It is assumed that the pipeline has one fixed end and the other free end, and is buried horizontally in the un-liquefiable topsoil upper the saturated liquefiable layer and subjected to the ground subsidence uniformly distributed along the pipeline axis. Figure 5 shows the typical characteristic of soil spring used in this study. In the liquefaction analysis by NUW2 the stiffness of the soil is related with the effective stress ratio. The soil spring to the pipeline may be also related to the effective stress ratio. Figure 6 shows such relation between the soil spring and the effective stress in which both parameters are represented by the ratio to the initial one. For pipeline analysis we determine the soil spring from the following equation;

$$k / k_0 = \sqrt{\sigma'_v / \sigma'_{v0}} \tag{15}$$

where k, k_0 are the soil springs during liquefaction analysis and initial one, respectively; σ'_v, σ'_{v0} are the effective stress during liquefaction analysis and initial one, respectively; k_0=2.918x10^2(kN/m^2) (N-value of soil:7). The symbolic marks of circle and rectangle in Figure 6 are obtained by the experiment for pipeline model during liquefaction process [Akiyoshi *et al.* 1989]. Figures 7 and 8 show the characteristics of the S-type and GM-type joints, respectively, in which (a) and (b) represent the rotational and axial characteristics, respectively.

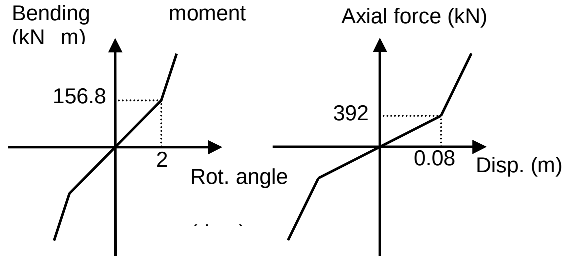

(a) Rotational joint spring (b) Axial joint spring

Figure 7: Characteristics Of S-Type Joint

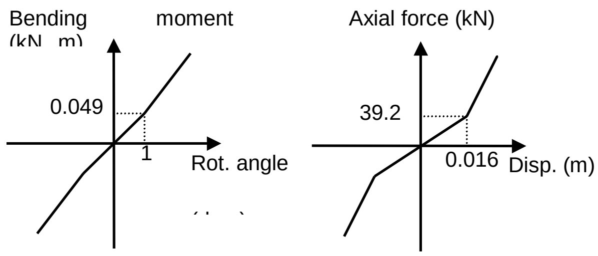

(a) Rotational joint spring (b) Axial joint spring

Figure 8: Characteristics Of Gm-Type Joint

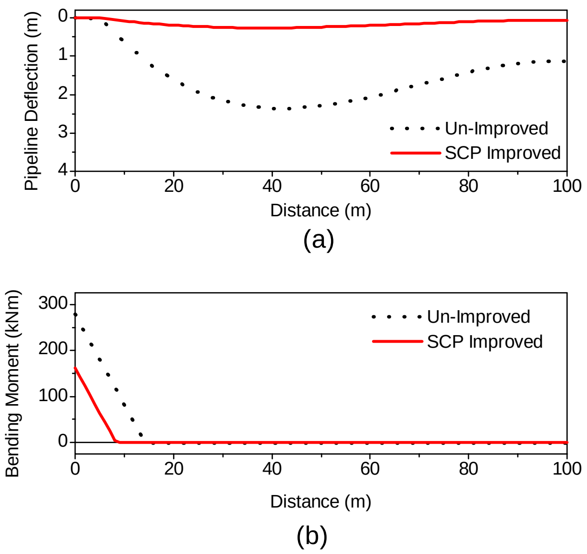

Figure 9: Distribution Of Pipeline Response (S-Type Joint)

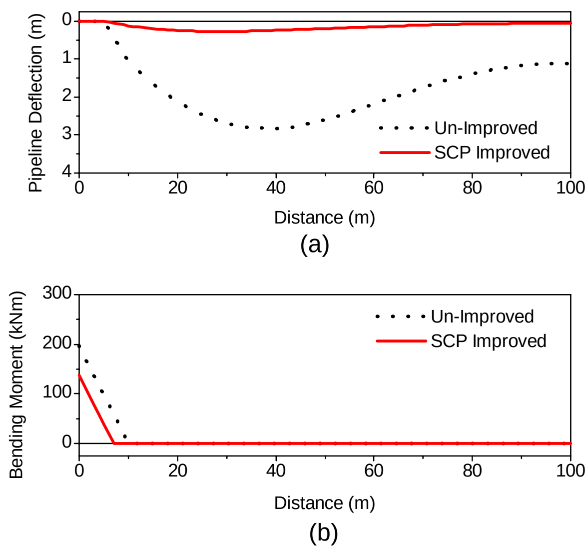

Figure 10: Distribution Of Pipeline Response (Gm Type Joint)

Results of pipeline response subjected to subsidence displacement of model ground

Figures 9 and 10 show the distribution of the deflection and bending moment responses of the pipeline with S-type joint and GM type joint, respectively, which is subjected to the ground subsidence. In each Figure the solid line and dotted one show the responses for the maximum input ground displacement 1.1m of un-improved case and 0.06m of improved one, respectively. In Figures 9 and 10, the maximum deflection responses of pipeline buried in the SCP-improved ground are reduced below 1/8 the responses of un-improved case, and the bending moment concentrates in near the fixed end (the left side in Figures) of the pipeline.

Figures 11 and 12 show the responses of the buried pipelines with S-type joint and GM-type one, respectively, and in which (a), (b) and (c) show the maximum responses of the pipeline deflections, joint rotational angles and bending moments, respectively, versus the ground model number as shown in Table 1. In these Figures, the symbolic marks of black circle and white one represent the responses of the pipeline subjected to the ground subsidence in the cases of un-improved ground and improved one, respectively. Since the bigger number of the model ground means the thickness H2 of liquefied layer in Table 1 thinner, the responses of pipeline deflection and joint rotational angle decrease as the number of model ground increases. But for the maximum bending

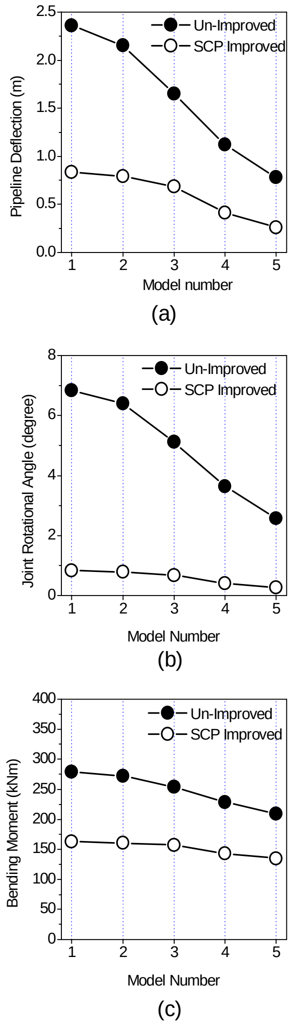

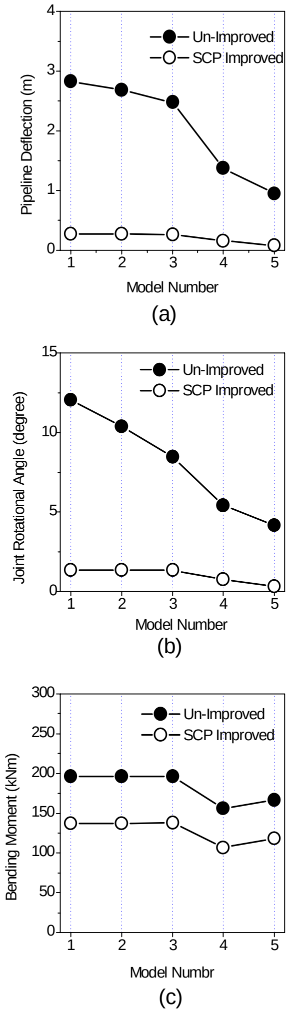

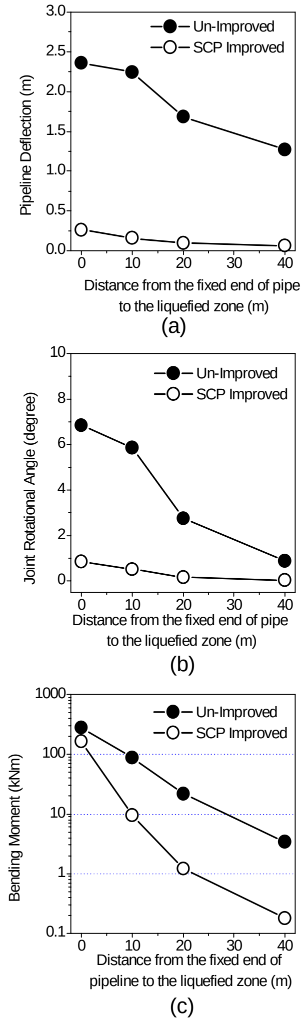

Figure 11: Maximum Pipeline Response (S-Type Joint)

Figure 12: Maximum Pipeline Response (Gm Type Joint)

Figure 13: Maximum Pipeline Response (S-Type Joint)

moment response keeps almost same level versus the ground model number. Figures 11 and 12 show that the SCP improvement is effective to reduce the responses of pipelines during seismic excitation.

Figure 13 show the responses of the pipelines with S-type joint versus the distance from the fixed end of pipeline to the liquefied zone, and in which (a), (b) and (c) represent the same maximum pipeline responses as shown in Figures 11 and 12. If the fixed end of the pipeline is included in the liquefied zone which means the distance 0m of the horizontal axis in Figure 13, the maximum pipeline deflection over 2.0m and the joint rotational angle over 5.0 degree may cause the damage of the pipeline. Increasing of the distance from the fixed end to the liquefied zone, the pipeline responses decrease and the possibility of the occurrence of the damage becomes lower.

CONCLUSIONS

In this paper we analyze the ground subsidence including the effect of the compacting ground improvement method and evaluate the responses of the pipeline subjected to the subsidence of the surface ground. The results obtained in this study are summarized as follows;

(1) The subsidence response evaluated by the proposed method is comparable with the observed subsidence of

the field case during Hyougoken-Nanbu Earthquake.

(2) SCP ground improvement is effective to prevent soil liquefaction and reduce the responses of the pipeline subjected to the ground subsidence induced by liquefaction.

(3) The responses of the pipeline subjected to the subsidence of liquefied ground are dependent to the distance from the fixed end of pipeline to the liquefied zone of the ground and increase, as the distance becomes short.

(4) The proposed method is useful not only to predict the response of pipeline buried in SCP improved ground but also to evaluate the effectiveness of countermeasures against liquefaction.

REFERENCES

Akiyoshi, T., Fuchida, K. *et al*. (1989), ”Estimation of restorning force characteristics of pipelines buried in liquefied ground”, *J. of Structures and Materials in Civil Engineering*, 5, pp39-46(in Japanese).

Akiyoshi, T., Fuchida, K. *et al*. (1993), ”Liquefaction analysis of sandy ground improved by sand compaction piles”, *Int. J. Soil Dynamics and Earthquake Engineering*, 12, 5, pp299-307.

Akiyoshi, T., Fuchida, K. *et al*. (1994), “Simulation of sand compaction pile method”, *Proceedings of 9th Japan Earthquake Engineering Symposium*, pp949-954.

Akiyoshi, T., Fuchida, K. *et al*. (1998), “Analysis of liquefied ground flow by potential head method”, *Proceedings of 10th Japan Earthquake Engineering Symposium*, pp1509-1514(in Japanese).

Fuchida, K. and Wang, L.R.L. (1993), “Parametric study of buried pipelines subjected to liquefied ground movements”, *Technical Report*, 8, *ODU LEE*.

Hamada, M. *et al.* (1986), *Study on liquefaction induced permanent ground displacemen*t, Association for the Development of Earthquake Prediction, pp1-87.

Hamada, M. *et al*. (1995), *The 1995 Hyogoken-Nanbu (Kobe) Earthquake : liquefaction, ground displacement and soil condition in Hanshin area*, Association for the Development of Earthquake Prediction.

Iai, S. *et al*. (1992), “Strain space plasticity model for cyclic mobility”, *Soils and Foundations*, *JSSMFE*, 32, 2, pp1-15.

Japan Road Association (1996), *Specifications for highway bridges, Part V Earthquake-resistant design*, JRA (in Japanese).

Japan Society of Civil Engineers (1994), *Reconnaissance report on the January 15, 1993 Kushiro-oki Earthquake, Hokkaido*, *JSCE*, pp2202-282 (in Japanese).

Yasuda, S. *et al*. (1992), “The mechanism and a simplified procedure for the analysis of permanent ground displacement due to liquefaction”, *Soils and Foundations*, JSSMFE, 32, 1, pp149-160.

Yasuda, S. *et al*. (1996), “Effect of soil improvement on ground subsidence due to liquefaction”, *Special Issue of Soils and Foundations, Japanese Geotechnical Engineering*, pp99-107.

Zienkiewictz, O.C. and Shiomi, T. (1984), “Dynamic behavior of saturated porous media: The generalized Biot’s formulation and its numerical solution”, *Int. J. Numerical and Analytical Method in Geomechanics*, l.8, pp71-96.